



# **A Force Torsor Analysis for a Turning Process in the Presence of Self-excited Vibrations**

Olivier Cahuc, Alain Gérard, Claudiu-Florinel Bisu, Constantin Ispas

## **► To cite this version:**

Olivier Cahuc, Alain Gérard, Claudiu-Florinel Bisu, Constantin Ispas. A Force Torsor Analysis for a Turning Process in the Presence of Self-excited Vibrations. *Journal of Applied Mechanics and Materials*, 2011, 62, pp.135-146. <10.4028/WWW.scientific.net/AMM.62.135>. <hal-00660834>

**HAL Id: hal-00660834**

**<https://hal.science/hal-00660834v1>**

Submitted on 17 Jan 2012

**HAL** is a multi-disciplinary open access archive for the deposit and dissemination of scientific research documents, whether they are published or not. The documents may come from teaching and research institutions in France or abroad, or from public or private research centers.

L'archive ouverte pluridisciplinaire **HAL**, est destinée au dépôt et à la diffusion de documents scientifiques de niveau recherche, publiés ou non, émanant des établissements d'enseignement et de recherche français ou étrangers, des laboratoires publics ou privés.



HAL Authorization

## **A Force Torsor Analysis for a Turning Process in the Presence of Self-excited Vibrations**

**Olivier CAHUC<sup>a</sup>, Alain GERARD<sup>a</sup>, Claudiu BISU<sup>b</sup>, Constantin ISPAS<sup>b</sup>,**

<sup>a</sup> *Université de Bordeaux and CNRS UMR 5295, 351, cours de la Libération, 33405 Talence cedex, France*

<sup>b</sup> *University Politehnica Bucharest, 313 Splaiul Independentei, 060042 Bucharest, Roumanie*

Correspondence should be addressed to Alain Gérard, alain.gerard@u-bordeaux1.fr

A testing device in turning including, a six-component dynamometer, is used to measure the complete torsor of the cutting actions in the case of self-excited vibrations. For the tests, the insert tool used is a TNMA 160412 type carbide not coated, without chip breaker. The machined material is a chrome molybdenum 42CrMo24-type alloy. The test workpieces are cylindrical and have a diameter of 120 mm and a length of 30 mm. For the first time, we present an analysis of forces and moments for different depths of cut and different feed rates.

### **1 Introduction**

In the three-dimensional cutting configuration, the mechanical actions torsor (forces and moments), is often truncated: the moments part of this torsor is neglected due to lack of adapted metrology [1, 2, 3]. Unfortunately, until now, the results on the cutting forces are almost still validated using platforms of forces (dynamometers) measuring the forces' three components. The actions torsor is thus often truncated because the torsor moment part is probably neglected for lack of access to an adapted metrology [4, 5]. However, forces and pure moments (or torque) can be measured [6]. Recently, an application consisting in six-component measurements of the actions torsor in cutting process was carried out in the case of high speed milling [7], drilling [8, 9], etc. Cahuc et al., in [10], present another use of this six-component dynamometer in an experimental study: taking into account of the cut moments allows a better machine tool power consumption evaluation. It allows a better approach of the cut [8, 11, 12] and thus allow us to reach new properties of the vibrations of the chip-tool-workpiece system in the dynamic case.

Moreover, the tool torsor has the advantage of being transportable in any point and, especially, at the tool tip point  $O$ . The following study is carried out in several stages, including two major ones. The first one is related to the analysis of forces. The second one is dedicated to determining the central axis and a first moments analysis to the central axis during the cut.

In paragraph 2 we present first the experimental device used and associated measurement elements. Paragraph 3 is devoted to the measurement of the cutting process actions. An analysis of the forces exerted during the cut process is performed. It allows us to experimentally establish several properties of the cutting actions resultant. The case of the moments at the tool tip point is also accurately examined. The central axis of the torque is required (paragraph 4). The existence of central axes highlighted from the multiple tests noticeably confirm the presence of moments at the tool tip point. In paragraph 5, we carry out more particularly the analysis of the moments at the central axis by studying the case the most sensitive to

vibrations ( $ap = 5$  mm,  $f = 0.1$  mm/rev). Before concluding, this study gives a certain number of properties and drives to some innovative reflexions.

## 2. Experimental Device

The experimental device presented in Figure 1 is a conventional lathe (Ernault HN 400). The machining system dynamic behaviour is identified using a three-direction accelerometer fixed on the tool. Two unidirectional accelerometers are positioned on the lathe and on the front bearing of the spindle, in order to identify the influence of this one during the cutting process. All the cutting actions (forces and torques at the tool tip point) are measured by a six-component dynamometer [6]. The instantaneous spindle speed is continuously controlled (with an accuracy of 1%) by a rotary encoder directly coupled with the workpiece. The connection is carried out by a rigid steel wire. The test workpieces are cylindrical and have a diameter of 120 mm and a length of 30 mm. The geometry of the support part holder was optimised by a finite element analysis (using SAMCEF® software) in order to confer a maximum rigidity to the unit. This procedure is described in [13]. Thus, under a load  $P = 1,000$  N, for material having a Young modulus  $E = 21.10^5$  N/mm<sup>2</sup>, the workpiece dimensions selected are:  $D_I = 60$  mm (diameter),  $L_I = 180$  mm (length) for a bending stiffness of  $7.10^7$  N/m (Figure 2). These values are within the higher limit of the stiffness zone acceptable for a conventional lathe [14, 15, 16].

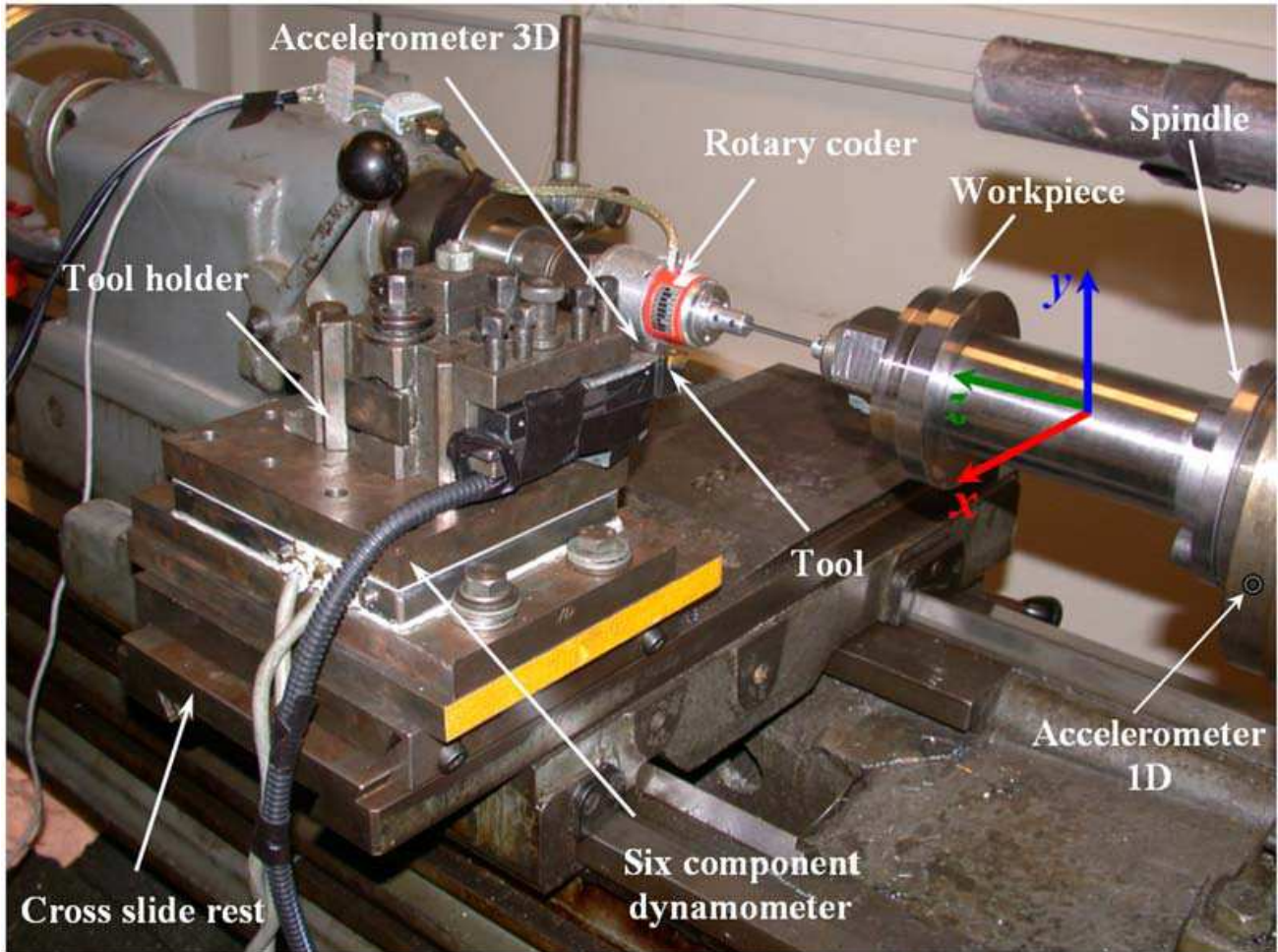


FIGURE 1: Experimental device and associated measurement elements.

During the tests, the insert tool used is a TNMA 16 04 12 type carbide not coated, without chip breaker. The machined material is a chrome molybdenum 42CrMo24-type alloy. Moreover, the tool geometry is characterized by the cutting angle  $\gamma$ , the clearance angle  $\alpha$ , the inclination angle of edge  $\lambda_s$ , the direct angle  $\kappa_r$ , the nozzle radius  $r_e$  and the sharpness radius  $R$  [17]. In order to limit the influence of the tool wear on measurements, the tool insert is examined after each test and changed if necessary ( $V_b \leq 0.2$  mm ISO 3685). Nevertheless, the present study does not, strictly speaking, deal with fretting and tool wear. The tool parameters are detailed in the Table 1.

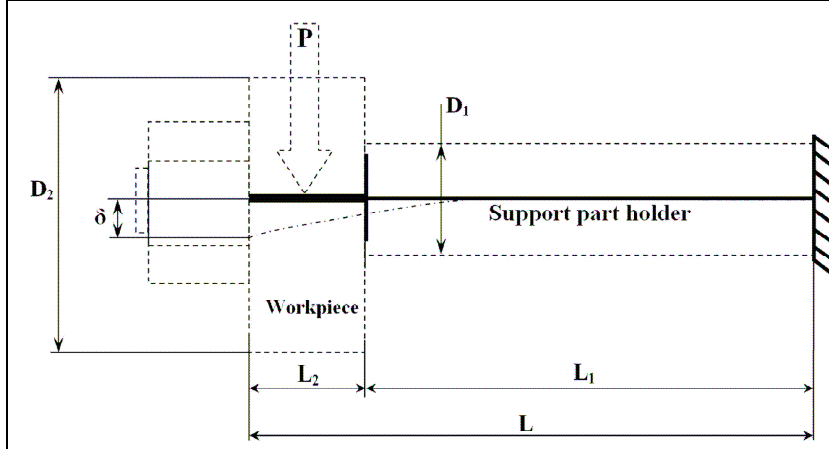


FIGURE 2: Geometry and dimension of the piece and the workpiece.

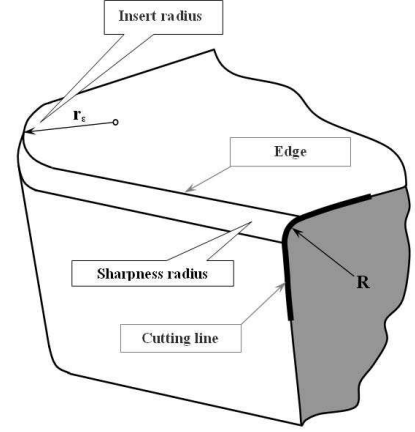


FIGURE 3: Tool geometry.

$\gamma$	$\alpha$	$\lambda$	$\kappa_r$	$r_e$	$R$
$-6^\circ$	$6^\circ$	$-6^\circ$	$91^\circ$	1.2 mm	0.02 mm

TABLE 1: Geometrical characteristics of the tool.

## 2 Cutting Torsor Actions

**3.1 Tests.** The experiments are performed within a framework similar to the one described in Cahuc et al., [10]. For each test, the complete torsor of the mechanical actions is measured using the six-component dynamometer according to the method initiated in Toulouse [18], developed by Cou  tard [11] and used in several occasions [7, 10, 19, 20, 21]. These mechanical actions are evaluated for four cut depths  $ap$  ( $= 1$  mm; 2 mm ; 3.5 mm ; 5 mm) and for four feed rates  $f$  ( $= 0.1$ ; 0.05; 0.0625; 0.075 mm/rev). The six-component dynamometer gives the instantaneous values of all the torque cutting components in the three-dimensional space ( $\mathbf{x}, \mathbf{y}, \mathbf{z}$ ) related to the machine tool (Figure 1). Measurements are performed in  $O'$ , which is the center of the six-component dynamometer transducer. Then, they are transported to the tool tip point  $O$  via the moment transport classical relations. Measurement uncertainties of the six-component dynamometer are:  $\pm 4\%$  for the force components and  $\pm 6\%$  for the moment components.

**3.2 Resultant of the cutting actions analysis.** For the four values feed rate  $f$  indicated above, two examples of forces resultant measurements applied to the tool tip point are presented: one of these for the stable case (quasi no-existent vibrations)  $ap = 2$  mm and another one for the unstable case (self-excited vibrations),  $ap = 5$  mm. The Figure 4 shows signals related to the resultant components of cutting forces following the three ( $x, y, z$ ) cutting directions. For the test case presented here, parameters used are:  $ap = 2$  mm,  $f = 0.1$  mm/rev and  $N = 690$  rpm. The Figure 5 shows signals related to the resultant components of cutting forces following the three ( $x, y, z$ ) cutting directions. For the test case here presented, parameters used are:  $ap = 5$  mm,  $f = 0.1$  mm/rev and  $N = 690$  rpm.

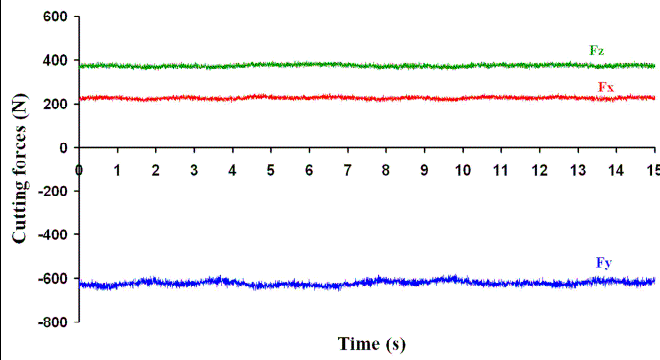


FIGURE 4: Signals related to the resultant components of cutting forces following the three ( $x, y, z$ ) cutting directions (without vibrations).

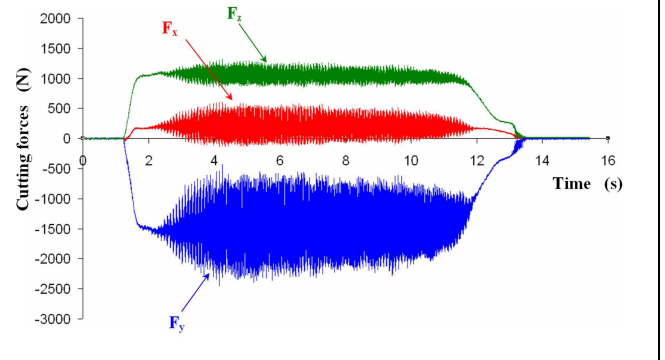


FIGURE 5: Signals related to the resultant components of cutting forces following the three ( $x, y, z$ ) cutting directions (with vibrations).

In the stable case ( $ap = 2$  mm,  $f = 0.1$  mm/rev), it appears (Figure 4) that the force component amplitudes remain almost independent of the time parameter. Thus, the amplitude variation is limited to 1 or 2 N around their rated values, starting with 200 N for ( $F_x$ ), 400 N for ( $F_z$ ), and 600 N for ( $F_y$ ). These variations are quite negligible and lower than uncertainties of measurements. Indeed, when the nominal rated stress is reached, the component noticed as the lowest value is ( $F_x$ ), while the highest in absolute value is ( $F_y$ ). Taking as reference the absolute value of ( $F_x$ ), the following relation between these three components comes:

$$|F_x| = |F_z|/2 = |F_y|/3 \text{ (stable case, } ap = 2 \text{ mm)}. \quad (1)$$

In the unstable case (Figure 5,  $ap = 5$  mm,  $f = 0.1$  mm/rev), we observe that the force component on the cutting axis ( $F_y$ ) has the most important average amplitude (1,500 N). It is also the most disturbed ( $\pm 1,000$  N) with oscillations between  $-2,450$  N and  $-450$  N. The force along the feed rate axis ( $F_z$ ) also has important average amplitude (1,000 N), but the oscillations are smaller:  $\pm 200$  N in absolute value and  $\pm 20\%$  in relative value. The efforts along the radial direction ( $F_x$ ) are the weakest in terms of average amplitude (200 N), but also the most disturbed regarding relative value ( $\pm 240$  N). These important oscillations are the tangible consequence of the contact tool/workpiece frequent ruptures and, thus, demonstrate the vibration and dynamical behaviour of the system **WTM**.

Finally, taking as reference the absolute value of ( $F_x$ ), the following relation between the absolute values of these three components comes:

$$|F_x| = |F_z|/5 = |F_y|/7.5 \text{ (unstable case, } ap = 5 \text{ mm)}. \quad (2)$$

In other words, whatever the cut depth  $ap$  we have the following order relation between the absolute values of the cutting actions components:

$$|F_x| \leq |F_z| \leq |F_y|. \quad (3)$$



More precisely, in the turning case studied here, whatever the cut depth  $ap = 2$  mm (stable case) or  $ap = 5$  mm (unstable case), we have, with the errors of experiments close the following relation between the absolute values of the cutting actions components:

$$|Fx| = |Fz|/ap = |Fy|/1.5ap. \quad (4)$$

So, the cutting actions are found proportional to the cut depth. This result is in agreement with [22, 23].

In the unstable case ( $ap = 5$  mm,  $f = 0.1$  mm/rev) the force resultant component highlights a plan in which a variable cutting forces  $F_v$  moves around a rated value  $F_n$  [23]. This variable force is an oscillating action (Figure 6) that generates tool tip displacements and maintains the vibrations of elastic system block-tool **BT** [23]. Thus, the cutting force variable and the self-excited vibrations of elastic **WTM** system are interactive, in agreement with research work [5, 15, 24, 25].

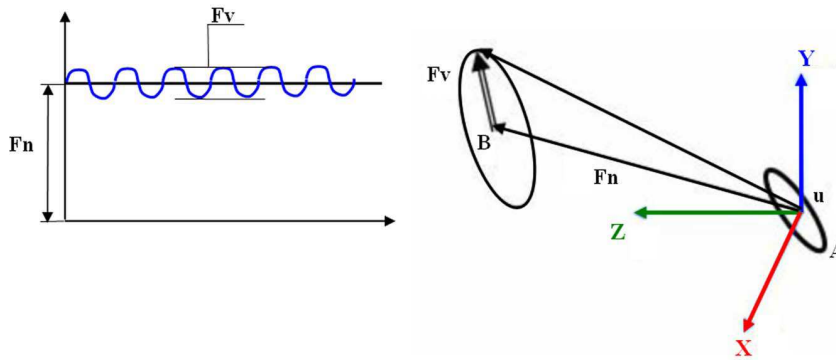


FIGURE 6: Cutting force  $F_v$  evolution around the nominal value  $F_n$ .

**3.2 Study of the moments to the tool point.** Like for the torsor resultant, we give here two examples of statements of the moment components to the tool point in the machine frame (Figure 1). The stable case is first presented, see Figure 7 (without vibrations following the three space machine directions in  $ap = 2$  mm and  $f = 0.1$  mm/rev), and then the unstable case is shown in Figure 8 (with vibrations following the three space machine directions  $ap = 5$  mm and  $f = 0.1$  mm/rev.).

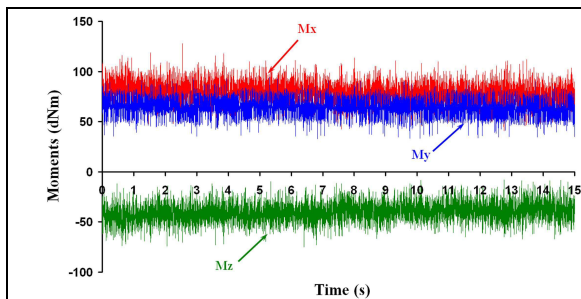


FIGURE 7: The moment components time signals that act on the tool tip ( $ap = 2$  mm).

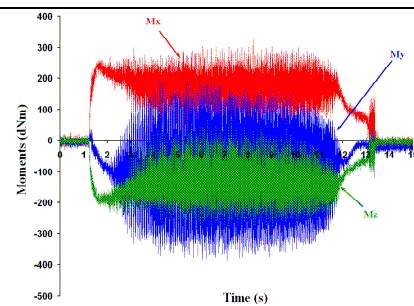


FIGURE 8: The moment components time signals that act on the tool tip ( $ap = 5$  mm).

Like for the resultants in the stable case (Figure 7), the moment components average values are slightly disturbed at the tool tip point (quasi-constants except for some dN.m – déci Newton metre –) though in the unstable case (Figure 8) the moment components average values are very disturbed at the tool tip point. However, we can note that the moment components at the tool tip point are more disturbed than their

equivalents regarding the resultant. Thus, the moment components seem more sensitive to the self-excited vibrations than the force components applied. Thus, the follow-up of those could be a good means of precociously detecting the existence of regenerative vibrations.

The analysis of the results shown in Figure 7 allows us to establish that, among the three moment components, the average value of the component along the axis feed rate is lowest ( $Mo_z = -40$  dN.m). It is the most disturbed in relative value ( $\pm 20$  dN.m i.e. 50%). The absolute value of the component along the axis of cut plays the role of pivot ( $Mo_y = 60$  dN.m) with a weaker disturbance in absolute value ( $\pm 16$  dN.m i.e. 30%). The highest component is along the radial axis ( $Mo_x = 80$  dN.m) with a weaker disturbance in absolute value ( $\pm 20$  dN.m i.e. 25%). Taking as reference the average values this of the component  $Mo_z$ , we have:

$$\|Mo_z\| = \|Mo_y\|/1.5 = \|Mo_x\|/2. \quad (5)$$

The analysis of the results shown in (Figure 8) allows us to establish that, among the three moment components, the average value of the absolute value of the component along the axis of cut is the lowest ( $Mo_y = -100$  dN.m). It is most disturbed in relative value ( $\pm 280$  dN.m i.e. variations of about 300%!). The component of the torque along the radial axis (x) is always positive  $Mo_x = 170$  dN.m ( $\pm 150$  dN.m); it is thus the most raised moment component and, proportionally, the least disturbed ( $\pm 75\%$ ). The  $Mo_z$  moment component along the radial direction is always negative with an average value about -140 dN.m in absolute value, the highest, but less disturbed than  $Mo_y$  (with oscillations of  $\pm 140$  dN.m i.e. only  $\pm 100\%$ ). Finally, for this cut depth, we have the following relation between the absolute values of the moment components:

$$\|Mo_y\| = \|Mo_z\|1.4 = \|Mo_x\|/1.7 \quad (ap = 5 \text{ mm}), \quad (6)$$

with a module of average torque at the tool tip point about  $\|Mo\| = 275$  dN.m. The comparison of Eq. (2) and Eq. (6), shows that the role of x and y axes is reversed for  $ap = 5$  mm. This allows us to think that the transport of the moments at the tool tip point has a major effect. Moreover, only the  $Mo_x$  modulus keeps the highest whatever the value of  $ap$  in the turning cases here considered. It is also the only positive and slightly decreasing component when the depth of cut increases. One notes that the components  $Mo_y$  and  $Mo_z$  are always negative when the cut depth increases. The modulus of the moments component at the tool tip point, increases with the cut depth, like the one of the resultant.

In the same way the general order relation (3) for the resultant is replaced for the moment at the tool tip point by:

$$|Mo_y| \leq |Mo_z| \leq |Mo_x|. \quad (7)$$

The x and y axes positions are also reversed regarding the resultant and moment at the tool tip point components. This can be allotted to the moments transport at the central axis. It is an additional incentive being studied of the moments at the central axis.

In addition, for the unstable case ( $ap = 5$  mm,  $f = 0.1$  mm/rev) the spatial evolution of the moments is no longer fully situated in a plane, as it is the case for forces. An 8, slightly out of plane is described (Figure 9) [27].

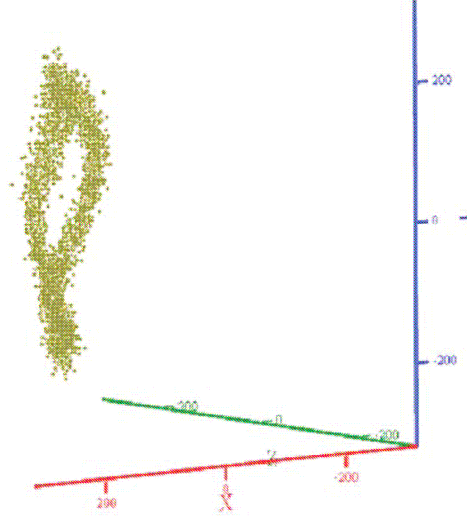


FIGURE 9: Moments place space representation.

### 3 Central Axis

It is well known that it is possible to associate a central axis to any torsor (except the torsor of pure moment), which is the single object calculated starting from the six torsor components [28]. A torsor  $[A]_O$  in a point  $O$  is composed of resultant forces  $\mathbf{R}$  and the resulting moment  $\mathbf{M}_O$

$$[A]_O = \left\{ \begin{array}{c} \vec{R} \\ M_o \end{array} \right. . \quad (8)$$

The central axis is the straight line classically defined by:

$$\overrightarrow{OA} = \frac{\vec{R} \wedge \overrightarrow{M_o}}{|\vec{R}|^2} + \lambda \vec{R}, \quad (9)$$

where  $O$  is the point where the mechanical actions torsor was moved (here, the tool tip) and  $A$  is the current point describing the central axis. Thus,  $\mathbf{OA}$  is the vector associated with the bi-point  $[O, A]$  (Figure 10). This line (Figure 10a) corresponds to the geometric points where the mechanical actions moment torsor is minimal. The central axis calculation consists in determining the points assembly (a line) where the torsor can be expressed according to a slide block (straight line direction) and the pure moment (or torque) [28].

The central axis is also the point where the resultant cutting force is colinear with the minimum mechanical moment (pure torque). The test results enable us to check, for each measurement point, if there is colinearity between the resultant cutting force  $\mathbf{R}$  and moment  $\mathbf{M}_A$  calculated at a point of the central axis (Figure 10b). The meticulous examination of the six mechanical action torsor components shows that the forces and the moment average values are not null. For each point of measurements, the central axis is calculated in the stable (Figure 11a) and unstable modes (Figure 11b). In any rigour, the case  $ap = 2$  mm and  $f = 0.1$  mm/rev should be described as quasi-stable movement because the vibrations exist but their amplitudes are very small —of the order of micrometres— thus, quasi null compared to the other studied cases. Considering the cutting depth value  $ap = 5$  mm and  $f = 0.0625$  mm/rev, the recorded amplitude was ten times more important.



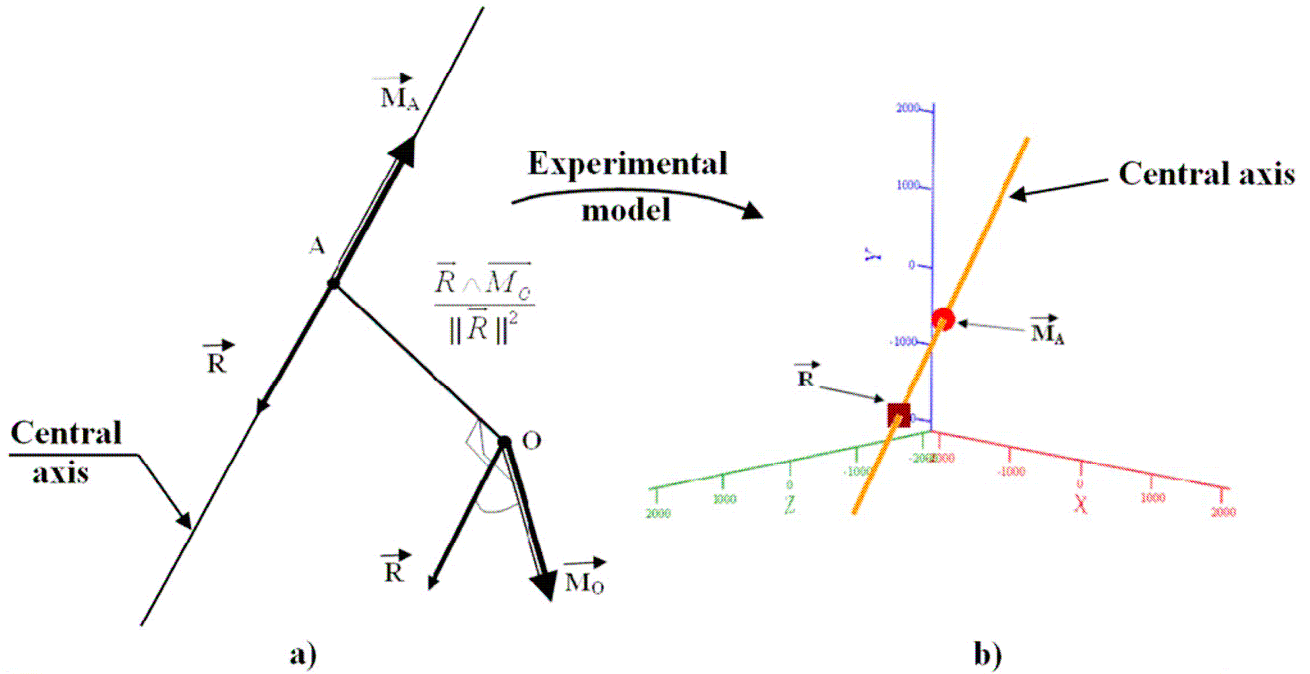


FIGURE 10. Central axis representation (a) and of the colinearity between vector sum  $\mathbf{R}$  and minimum moment  $\mathbf{M}_A$  at central axis (b).

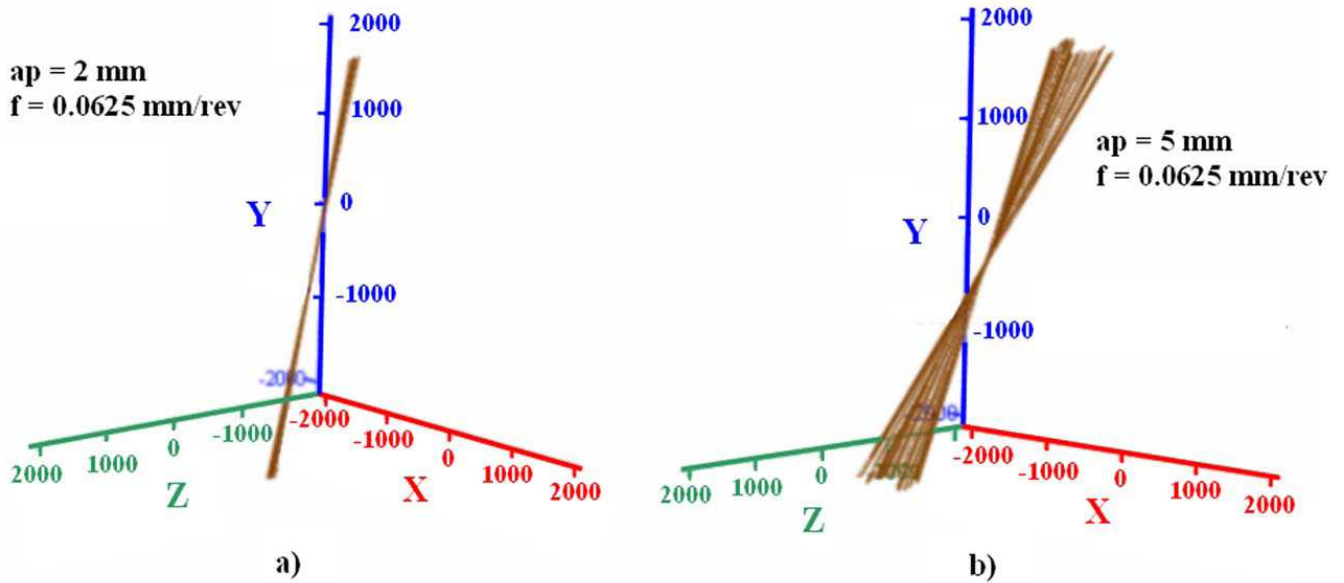


FIGURE 11: Central axes representation obtained for 68 spin rounds of the workpiece speed and feed rate  $f = 0.0625 \text{ mm/rev}$ ; a) stable process  $ap = 2 \text{ mm}$ ; b) unstable process  $ap = 5 \text{ mm}$ .

In the presence of vibrations ( $ap = 5 \text{ mm}$ ) for a 68 spin rounds of the workpiece (44 points of measurements per spin round), the dispersive character of the central axes beam, compared to the stable mode, can be observed, where this same beam is tightened more or less tilted compared to the normal axis on the plane ( $\mathbf{x}, \mathbf{y}$ ). The self-excited vibrations, due to the variable moment generation, can explain this central axis dispersion.

## 4 Analysis of Central Axis Moments Related

While transporting the moment from the tool tip at the central axis, the minimum moment (pure torque)  $\mathbf{M}_A$  is obtained. From the moment values at the central axis, constant and variable parts are deduced. Just like for the efforts, the variable part is due to the self-excited vibrations, as revealed below.

Using this decomposition, the moments contribution on the areas of contact tool–workpiece–chip is expressed. The observations resulting from the analysis show that the tool vibrations generate rotations; cause variations of contact; and, thus, generate variable moments, confirming the efforts analysis detailed in Section 3. This representation allows us to express the moments along the three axes of the machine tool: swivel moment in the  $y$  direction and the two moments of rotation along  $x$  and  $z$  directions.

For the unstable case, characterized by  $ap = 5$  mm and  $f = 0.1$  mm/rev, the analysis of the cutting torque components average values at the central axis (subscripted by the letter  $a$ ) leads to the following results:  $Max = -4$  dN.m  $\pm 24$  dN.m;  $May = -34$  dN.m  $\pm 160$  dN.m;  $Maz = 8$  dN.m  $\pm 110$  dN.m. Thus, one has the following relation between the modulus of the three torque components (with the errors of measurement close):

$$\|Max\| = \|Maz\|/2 = \|May\|/8. \quad (10)$$

The confrontation of Eq. (6) and (10) shows the importance of transporting the moment from the tool tip point to central axis. It is as also interesting to note as the module of the average couple of cut at the central axis is worth  $\|My\| = 88$  dN.m, three times less than at the tool point.

In addition, one notes that the torque modulus is increasing with feed rate as for the resultant cutting force, at the central axis. The moment component along the radial axis ( $x$ ) remains the weakest but also the least disturbed. Contrary to the moment components at the tool tip point or the resultant, the single order relations (3) and (8) are replaced by:

$$|Max| \leq |May| \leq |Maz| \quad \text{if } f \leq 0.0625, \quad (11)$$

$$|Max| \leq |Maz| \leq |May| \quad \text{if } f > 0.0625. \quad (12)$$

Depending on the feed rate, the role of cutting and feed rate axes is thus inversed. Moreover, the torque along the feed rate axis plays the role of “pivot”, and keeps it of the transportation at the tool tip point for  $f > 0.0625$ . When  $f \leq 0.0625$ , the role of “pivot” go back to the cutting axis, and the influence of cutting and the feed rate axes is inversed. This remark completes the previous one above, and highlights that the study of cutting moment at the central axis needs to be examined in more details.

## 5 Conclusion

Experimental procedures here developed allowed to determine the elements required for a rigorous analysis of the influence of tool geometry, its displacement, and the evolution of contacts tool/workpiece and tool/chip on the machined surface. These experimental results allowed us to establish a vectorial decomposition of actions analyzing the resultant of applied actions torsor during a turning process. Thus, it is demonstrated that the cutting effort evolves around a constant frated value, describing an “8” in a leaning plan compared with the machine spindle. This cutting force, whose application point describes an ellipse, is perfectly well correlated with displacements of the tool tip point, in a good agreement with [27].

Furthermore, a really innovative study of the moments at the tool tip point, and at the central axis of the action torsor, is presented. For the resultant like for the moment, at the tool tip point or the central axis, the modulus of these elements is increasing with the feed rate. An order relation exists between the average values of modulus of action components and the average values of moments at tool tip point. One notes especially that the roles of  $x$  and  $y$  axes are inversed, and  $z$  axis plays the role of “pivot”. But not unique order relation exists at the central axis. Only the moment modulus along the radial axis remains the weakest when

the feed rate increases. This property is common with the component modulus of the same row of the resultant. For the module of the other components of the moments at the central axis, their relative position depends on the feed rate value. This highlights that the study of cutting moments at the central axis needs to be examined in more details.

## References

- [1] K. Mehdi, J-F. Rigal and D. Play, "Dynamic behavior of thin wall cylindrical workpiece during the turning process, Part 2: Experimental approach and validation", *J. Manuf. Sci. and Engng.*, vol. 24, pp. 569-580, 2002.
  - [2] S. Yaldiz and F. Ünsacar, "Design, development and testing of a turning dynamometer for cutting force measurement", *Mat. and Des.*, vol. 27, pp. 839-846, 2006.
  - [3] S. Yaldiz and F. Ünsacar, "A dynamometer design for measurement the cutting forces on turning", *Measurement*, vol. 39, pp. 80-89, 2006.
  - [4] E. Marui, S. Ema and S. Kato, "Chatter vibration of the lathe tools. Part 2 : on the mechanism of exciting energy supply" *J. of Engng. for Indust.*, vol. 105, pp. 107-113, 1983.
  - [5] R. J. Lian, B. F. Lin and J. H. Huang, "Self-organizing fuzzy control of constant cutting force in turning", *Int. J. Adv. Manuf. Technol.*, vol. 29, pp. 436-445, 2007.
  - [6] Y. Couétard, French patent – CNRS – 93403025.5 N° 2240, 1993.
  - [7] Y. Couétard, O. Cahuc and P. Darnis, "Mesure des 6 actions de coupe en fraisage grande vitesse" Third in *Proceedings of the Int. Conf. on Met. Cut. and High Speed Machin.* pp. 37-42, – Metz, 27-29 juin 2001.
  - [8] S. Laporte, J-Y. K'nevez, O. Cahuc and P. Darnis, "Phenomenological model for drilling operation" *Int. J. Adv. Manuf. Technol.*, vol. 40, n° 1-2, pp. 1-11, 2009, doi: 10.1007/s00170-1305-4.
  - [9] S. Yaldiz, F. Ünsacar, H. Saglam and H. Isik, "Design, development and testing of a four-component milling dynamometer for the measurement of cutting force and torque", *Mech. Syst. and Sign. Proces.* vol. 21, pp. 1499-1511, 2007.
  - [10] O. Cahuc, P. Darnis, A. Gérard and J-L. Battaglia, "Experimental and analytical balance sheet in turning applications", *Int. J. Adv. Manuf. Technol.*, vol. 29, pp. 648-656, 2001.
  - [11] Y. Couétard, "Caractérisation et étalonnage des dynamomètres à six composantes pour torseur associé à un système de forces", Ph. D. Thesis, Université Bordeaux1, 2000.
  - [12] C. F. Bisu, P. Darnis, J-Y. K'nevez, O. Cahuc, R. Laheurte, A. Gérard and C. Ispas, "Nouvelle analyse des phénomènes vibratoires en tournage", *Méc. & Indust.* vol. 8, pp. 497-503, 2007.
  - [13] C. F. Bisu, Ph. D. Thesis, "Etude des vibrations auto-entretenues en coupe tridimensionnelle: nouvelle modélisation appliquée au tournage", Université Bordeaux 1 and Universitatea Politehnica Bucharest, 2007.
  - [14] C. Ispas, H. Gheorghiu, I. Parausanu and V. Anghel, "*Vibrations des systèmes technologiques*". Agir, Bucarest, 1999.
  - [15] F. Koenigs, J. Tlustý, "*Machine Tools Structures*". Pergamon Press 1970.
  - [16] W. Konig, E. Sepulveda, H. Lauer-Schmaltz, "Zweikomponenten schnittkraftmesser". Industrie-Anzeiger, 1997.
  - [17] R. Laheurte, "Application de la théorie du second gradient à la coupe des matériaux", Ph. D. Thesis, Université Bordeaux 1, 2004.
  - [18] D. Toulouse, "Contribution à la modélisation et à la métrologie de la coupe dans le cas d'un usinage tridimensionnel", Ph. D. Thesis, Université Bordeaux 1, 1998.
  - [19] P. Darnis, O. Cahuc and Y. Couétard, "Energy balance with mechanical actions measurement during turning process", in *Proceedings of the Int. Sem. on Improv. Mach. Tool Perfor.*, 3-5 July - La baule, 2000.
  - [20] R. Laheurte, P. Darnis and O. Cahuc, "Evaluation de l'énergie mise en jeu et du comportement des outils de coupe dans l'usinage", in *Proceedings of the IDMME 02*, 14-16 Mai – Clermont Ferrand, 2002.
-

- 
- [21] R. Laheurte, O. Cahuc, P. Darnis and J-L. Battaglia, “Metrological devices in cutting process”, in *Proceedings of the 6<sup>th</sup> Int. ESAFORM*. 28-30 April - Salerno 2003.
  - [22] P. G. Benardos, S. Mosialos, and G. C. Vosniakos, “Prediction of workpiece elastic deflections under cutting forces in turning”, *Rob. Comput. Integ. Manuf.* vol. 22, pp. 505-514, 2006.
  - [23] C. F. Bisu, A. Gérard, J-Y. K'nevez, R. Laheurte and O. Cahuc, “Self-excited vibrations in turning: forces torsor analysis”, *Int. J. Adv. Manuf. Technol.* vol. 44, n°5-6, 2009, doi: 10.1007/s00170-008-1850-5.
  - [24] Sr. D. E. Dimla, “The impact of cutting conditions on cutting forces and vibration signals in turning with plane face geometry inserts”, *J. Mat. Proc. Tech.*, vol. 155-156, pp. 1708-1715, 2004.
  - [25] G. Stawell Bal, “*A treatise on the theory of screws*”, Cambridge University Press, London, 1900.
  - [26] U. Seker, A. Kurt and I. Ciftci, “The effect of feed rate on the cutting forces when machining with linear motion”, *J. Mat. Proc. Tech.*, vol. 146, pp. 403-407, 2004.
  - [27] C. F. Bisu, P. Darnis, A. Gérard and J-Y. K'nevez, “Displacements analysis of self-excited vibrations in turning”, *Int. J. Adv. Manuf. Technol.* vol. 44, n° 1-2, pp. 1-16, 2009, doi: 10.1007/s00170-008-1815-8.
  - [28] P. Brousse, “*Cours de mécanique (1er cycle et classe prépa.)*”, Armand colin, Paris, 1973.

### Acknowledgements

The authors would like to thank the French “Ministère des Affaires étrangères et européennes” for the financial support of this project under the program ECO-NET project N° 21367XL. This paper was also supported by CNCSIS-UEFISCSU, project PNII-RU-code-194/2010

---